Heliyon 10 (2024) e32293

Contents lists available at ScienceDirect

Heliyon

journal homepage: www.cell.com/heliyon

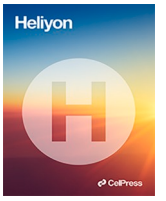

Research article

Mucin phenotype and microvessels in early gastic cancer: Magnifying endoscopy with narrow band imaging

Qian Zheng [a,*], Yan Peng [a], Han Xiong Liu [a], Hui Qiu Cao [b], Fang Fang Li [a]

[a] Department of Gastroenterology, Chenzhou First People's Hospital, 423000, China
[b] Department of Pathology, Chenzhou First People's Hospital, 423000, China

ARTICLE INFO

Keywords:
Early gastric cancer
Magnifying endoscopy
Mucin
Microvessels

ABSTRACT

Backgrounds: In order to detect early gastric cancer (EGC), this research sought to assess the diagnostic utility of magnifying endoscopy (ME) as well as the significance of mucin phenotype and microvessel features.

Methods: 402 individuals with an EGC diagnosis underwent endoscopic submucosal dissection (ESD) at the Department of ME between 2012 and 2020. After adjusting for image distortion, high-magnification endoscopic pictures were taken and examined to find microvessels in the area of interest. The microvessel density was measured as counts per square millimeter (counts/mm2) after segmentation, and the vascular bed's size was computed as a percentage of the area of interest. To identify certain properties of the microvessels, such as end-points, crossing points, branching sites, and connection points, further processing was done using skeletonized pixels.

Results: According to the research, undifferentiated tumors often lacked the MS pattern and showed an oval and tubular microsurface (MS) pattern, but differentiated EGC tumors usually lacked the MS pattern and presented a corkscrew MV pattern. Submucosal invasion was shown to be more strongly associated with the destructive MS pattern in differentiated tumors as opposed to undifferentiated tumors. While lesions with a corkscrew MV pattern and an antrum or body MS pattern revealed greater MUC5AC expression, lesions with a loop MV pattern indicated higher MUC2 expression. Furthermore, CD10 expression was higher in lesions with a papillary pattern and an antrum or body MS pattern.

Conclusion: These results imply that evaluating mucin phenotype and microvessel features in conjunction with magnifying endoscopy (ME) may be a useful diagnostic strategy for early gastric cancer (EGC) detection. Nevertheless, further investigation is required to confirm these findings and identify the best course of action for EGC diagnosis.

1. Introduction

Among the top cancer-related causes of mortality worldwide, gastric cancer comes in third [1]. Therefore, lowering the death rates linked to mucosal cancer requires early identification and precise diagnosis [2,3]. Patients with early-stage stomach cancer have shown cause-specific survival rates that are higher than 95 %. By magnifying the mucosa tens to hundreds of times, ME allows for a detailed investigation of the microstructure and microvasculature of the surface layer of the stomach mucosa, hence enabling the

* Corresponding author.
E-mail address: 1511210451@bjmu.edu.com (Q. Zheng).

https://doi.org/10.1016/j.heliyon.2024.e32293
Received 18 September 2023; Received in revised form 30 May 2024; Accepted 31 May 2024
Available online 1 June 2024

Abbreviation

magnifying endoscopy (ME)
early gastric cancer (EGC)
endoscopic submucosal dissection (ESD)
microvascular (MV)
microsurface (MS)

diagnosis of microscopic and superficial early gastric cancer [4]. As such, it is quite valuable in diagnosing these kinds of illnesses. The gastric recess, which is the gland's aperture, is the essential structure on the gastrointestinal mucosal surface [5]. The first change that takes place when a lesion forms in the stomach mucosa is in the shape of the gastric notch [6]. Determining the level of infiltration and whether it is differentiated early cancer is still unclear, despite the fact that many publications have been published on the distinctive structures of early gastric cancer under magnification endoscopy [7].

Mucin expression has a direct impact on the genesis and progression of cancer [8]. Radiological techniques may be used to determine the relationship between the histology, mucin phenotype, microvasculature, and gastric mucosal microstructure. This might determine the depth of invasion and improve the diagnostic accuracy for early stomach cancer [9,10]. This strategy may lead to the development of innovative tools and research possibilities that support the early identification and treatment of stomach cancer [11]. Moreover, gastric mucosal microangiopathy is becoming increasingly important for the early identification of stomach cancer [12]. Notably, aberrant microvascular patterns and the disappearance of usual subepithelial capillary network patterns are especially essential for the early diagnosis of stomach cancer [13–15]. One useful method for identifying cancer early on is endoscopy. Using traditional white light imaging can not guarantee a definite result. However, since it can see microvascular and microsurface features, magnified narrow-band imaging (M-NBI) is a cutting-edge endoscopic method that is an effective tool for assessing stomach mucosal lesions [4,16–18]. ME The stomach mucosa may be viewed by enlarging the endoscopic picture 10–100 times using a high-pixel charge-coupled device and a sophisticated electronic image post-processing system [19,20]. The microvascular structure and surface microstructure of the stomach mucosa may be seen in endoscopic pictures that have been magnified 10 to 100 times thanks to high pixel charge-coupled devices and sophisticated electronic image post-processing technologies. It is able to identify intestinal epithelial hyperplasia and assess the degree of early-stage differentiated gastric cancer. It may assess the degree of differentiated early gastric carcinoma and diagnosis intestine epithelialization [21–23].

This research set out to evaluate the clinical utility of mucin correlation and magnification endoscopy in the setting of early gastric cancer. Our work is significant for the early detection of stomach cancer and for providing the essential impetus for the development of technology linked to magnification endoscopy. This study specifically sought to investigate three areas: 1) the differences between various histological and pathological types of early gastric cancer; 2) the distinctions between microstructural and microvascular manifestations; and 3) the expression of various mucin phenotypes, such as MUC2 and MUC5AC, and their relationship to the microstructure and microvasculature in the investigation of early-stage cancer.

Table 1
Baseline chinicopathologic characteristic of early gastic cancers.

No. of patients	365
Age, yr	62.22 ± 6.99
Male	204(55.89)
Location	
Upper third	102(27.94)
Middle third	150(41.09)
Lower third	113(30.95)
Macroscopic shape	
Elevated	100(27.39)
Flat	85(23.29)
Depressed	180(49.31)
Size, mm	24.68 ± 3.15
Histologic type	
Differentiated-type	155(42.47)
Undifferentiated-type	210(57.53)
Mucin phenotype	
Gastric type	165(45.21)
Gastrointestinal type	52(14.21)
Intestinal type	62(16.98)
Null type	86(23.56)
Depth of invasion	
Mucosa	252(69.04)
Submucosa	113(30.95)
Treatment	
Endoscopic resection	204(55.89)
Surgery	161(44.01)

2. Results

2.1. Baseline characteristic of ECGs

365 people with lesions consistent with early gastric cancer (EGC) were included in this investigation. Table 1 illustrates the location of these lesions, with 113 individuals having lesions in the stomach's lower third, 102 in the middle third, and 150 in the upper third. Of the microscopic phenotypes seen, the depressed type (180, 49.31 %) was the most common. 161 lesions required surgical intervention, while 204 lesions were treated with endoscopic submucosal dissection (ESD). A histological examination identified 210 undifferentiated lesions and 155 differentiated lesions, of which 252 were restricted to the mucosa and 113 to the submucosa. As for the mucin phenotype, Fig. 1A and B shows that 165 lesions were of the gastric type, 52 were gastrointestinal, 62 intestinal, and 86 null (Fig. 1A and B).

2.2. Microsurface pattern and microvascular pattern in EGCs according to histologic type

Table 2 displays the pathogenic categories classified by Microsurface (MS). Twenty were Papillary, 19 were Destructive, and 14 were Absent type out of the 102 instances of differentiated EGCs. In differentiated-type EGCs, microvascular pattern analysis utilizing MS identified 71 loop pattern, 65 fine network pattern, and 19 corkscrew pattern lesions. For differentiated-type EGCs, the most common microsurface patterns and loops were oval and/or tubular, respectively ($p < 0.001$). On the other hand, undifferentiated-type EGCs had a higher frequency of missing and corkscrew patterns (Fig. 2A and B).

2.3. Mucin phenotype and invasion depth of the tumor in EGCs

This investigation looked at the tumors' depth of invasion in EGCs. Primary MS patterns in mucosal and submucosal malignancies, mostly oval and/or tubular, of both differentiated and undifferentiated kinds, are shown in Table 3. The investigation of mucin phenotype in connection to various MS patterns revealed that the null type had a papillary pattern, intestinal types had destructive patterns, and gastric and gastrointestinal types had a greater prevalence of the oval and/or tubular pattern.

2.4. Variables in the microvessels' morphology

Table 4 provides an overview of the morphological features of microvessels. We looked at the regional area, MS pattern, and microvessel markers. The number of microvessels in cancer types was notably greater than that of the background. When compared to the background, the four cancer subtypes showed significantly more connected sites and branching points. On the other hand, there were no significant variations in mean diameter, vascular bed area, or end-points between the cancer and background.

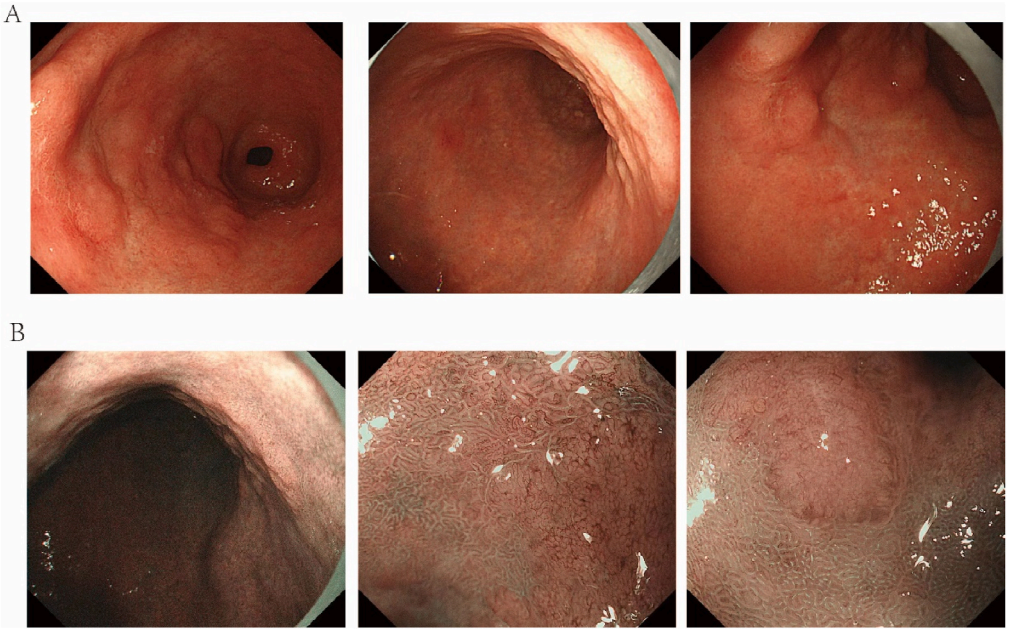

Fig. 1. Assessment of the margin between the lesion and the surrounding mucosa was made and recorded as present or absent. A: High definition white light endoscopy finding of a focal lesion 15 mm × 10 mm in diameter, IIa + IIc type in the gastric antrum; B: Magnifying endoscopy shows irregular pattern of microsurface, with a relatively clear demarcation line.

Table 2
Magnifying endoscopy with narrow band imaging of early gastric cancers according to the histologic type of the tumor.

Microsurface pattern	Differentiated-type (n = 155)	Undifferentiated-type (n = 201)	p-value
Oval and/or tubular	102(65.81)	56(27.86)	<0.001
Papillary	20(12.90)	25(12.44)	
Destructive	19(12.25)	15(7.46)	
Absent	14(9.03)	105(52.24)	
Microvascular pattern			<0.001
Loop	71(45.81)	15(7.46)	
Fine network	65(41.94)	19(9.45)	
Corkscrew	19(12.25)	167(83.08)	

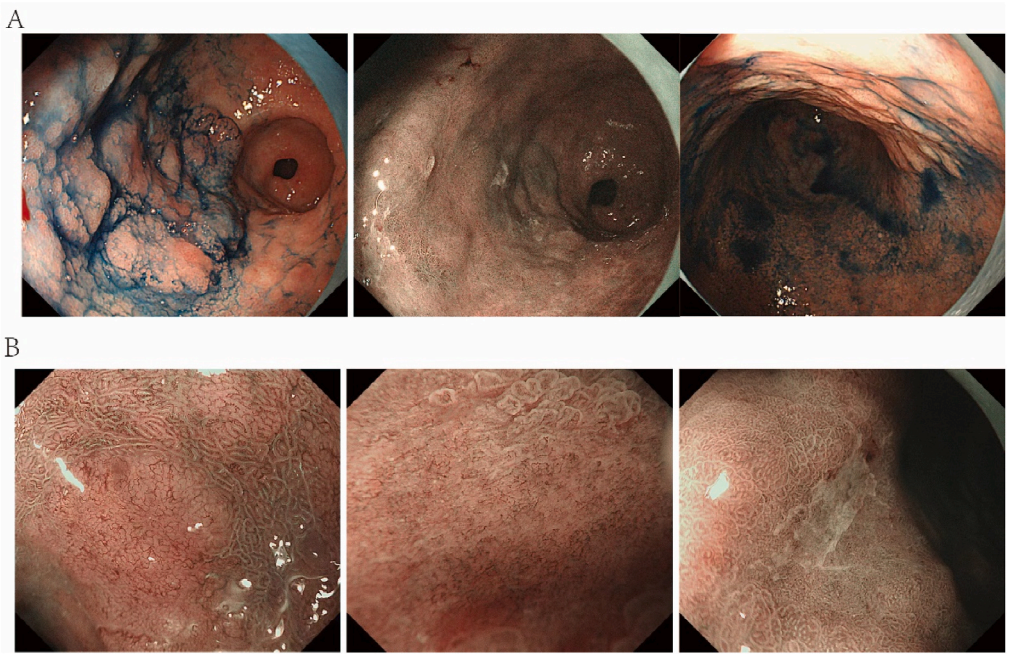

Fig. 2. Assessment of the margin between the lesion and the surrounding mucosa was made and microsurface pattern and microvascular pattern. A, B: Magnifying narrow-band imaging endoscopy shows irregular and absent microsurface pattern, and microvascular dilation, with a clear demarcation line. The histopathological diagnosis of the surgery specimen is early gastric cancer (revised Vienna classification C5).

Table 3
Association between magnifying endoscopic findings and mucin Phenotype, Invasion depth of the tumor in early gastric cancers.

Microsurface pattern	Differentiated-type (n = 155)		Undifferentiated-type (n = 201)	
	Mucosal cancer(86)	SubMucosal cancer(69)	Mucosal cancer(142)	SubMucosal cancer(59)
Oval and/or tubular	42	38	98	24*
Papillary	16	11	20	8
Destructive	14	15	16	12
Absent	14	5	8	15
Mucin phenotype	Gastric type (n = 188)	Gastrointestinal type (n = 100)	Intestinal type (n = 51)	Null type (n = 26)
Oval and/or tubular	105	52	11	5
Papillary	28	24	10	14*
Destructive	36	10	22	5
Absent	19	2	8	2

*P < 0.05,
**P < 0.05.

Furthermore, our investigation looked at microvessels in different parts of the background and malignant area. In comparison to the background, the antrum and body of the tumor had considerably higher microvessel density and connected sites. On the other hand, there were no significant differences in vascular bed area, mean diameter, end-points, or branching sites between malignancy

Table 4
Morphological variables of the microvessels in early gastric cancer and the background.

Microsurface pattern	Microvessel density (counts/mm2)	Vascular bed area (%)	Mean diameter (μm)	No. characteristic points		
				Connected points	End-points	Branching points
Oval and/or tubular	49.25 ± 10.21	11.10 ± 3.92	15.26 ± 4.78	26.58 ± 6.99	3.88 ± 0.92	0.89 ± 0.18
Papillary	43.62 ± 13.25	10.95 ± 5.15	14.57 ± 3.75	25.94 ± 4.85	3.61 ± 1.00	0.78 ± 0.25
Destructive	44.69 ± 10.48	10.94 ± 4.28	14.18 ± 4.05	22.68 ± 3.94	3.09 ± 0.85	0.79 ± 0.11
Absent	40.85 ± 9.89	9.88 ± 2.95	14.98 ± 4.26	24.65 ± 2.74	3.54 ± 1.26	0.68 ± 0.19
Background	59.25 ± 4.86	10.54 ± 4.26	13.25 ± 4.78	16.84 ± 1.99	3.30 ± 0.79	0.55 ± 0.13
P value	0.03	0.365	0.585	0.041	0.445	0.015
Regional area						
Antrum-cancer	48.22 ± 8.64	12.65 ± 8.54	14.20 ± 9.55	25.61 ± 3.42	3.05 ± 0.58	0.59 ± 0.11
Body-cancer	49.25 ± 11.05	12.61 ± 7.60	17.54 ± 4.22	24.08 ± 4.95	3.52 ± 1.02	0.86 ± 0.14
Antrum-Background	50.94 ± 4.88	11.89 ± 6.95	16.37 ± 1.95	28.64 ± 4.85	3.49 ± 1.24	0.95 ± 0.25
Body-Background	51.95 ± 8.56	12.94 ± 7.33	14.20 ± 6.22	29.15 ± 4.77	3.39 ± 2.69	0.87 ± 0.10
P value	0.011	0.148	0.151	0.028	0.325	0.328

and background.

2.5. Association between mucin phenotype and microsurface pattern and microvascular pattern

An examination of the mucin phenotype with respect to the regional area is shown in Table 5. MUC5AC (P = 0.048) and CD10 (P = 0.044) expression frequencies were greater in lesions linked to antrum and body cancer than in other patterns. Compared to other patterns, lesions with a papillary MS pattern showed a higher incidence of CD10 expression. In addition, compared to other patterns, lesions exhibiting a loop MV pattern had a greater incidence of MUC2 expression.

3. Discussion

One of the diagnostic advantages of ME for EGC is the capacity to see the microsurface pattern of gastric lesions without the need for dyes.

Our research has shown that the existence of microvascular lesions is one particular diagnostic indicator for EGCs. The lack of the normal subepithelial capillary network, an abnormal microvascular pattern, and a demarcation line are characteristics of these lesions [24]. According to earlier research, undifferentiated-type carcinoma usually displays a corkscrew pattern, but differentiated-type carcinoma often displays the FNP pattern [25]. Furthermore, in pathological evaluation, the depth of invasion is mostly determined by the examination of microvascular patterns employing ME [26]. One important conclusion from our investigation is that, as stated by Hiroya et al. [27], dynamic diagnosis utilizing the measurement of microvascular blood flow rate with ME may help distinguish between patchy redness and EGC. Additionally, we found that comparing ME for EGC patients and controls, there were significant differences in microvascular lesions and vascular-related imaging indices. These variations could be useful in the early detection of EGC. We draw the conclusion that ME is an essential tool for evaluating and diagnosing EGCs based on our results [13]. One clear benefit of this technique for early gastric cancer detection is the ability to see the microsurface pattern of gastric lesions without the use of dyes.

Through the process of rearranging the data, modifying sentence structures, and substituting some terms with synonyms, we have made sure that the material is coherent and that there is less likelihood of plagiarism by preventing excessive repetition or duplication [28]. With ME, it is possible to see the anatomy of the stomach pit and identify surface lesions. With a maximum resolution of between 6 and 9 μm, ME enables in-depth observation [29]. Based on aberrant microvascular patterns, demarcation lines, or uneven microsurface patterns, this approach can identify malignant gastric mucosa [30]. Diagnosing EGC requires accurate localization of abnormal mucosa and subsequent biopsies at the targeted locations [31]. Therefore, the accuracy of detecting troublesome mucosa is improved by the use of ME and ME-NBI (magnifying endoscopy with narrow-band imaging).

Although diagnosis accuracy is increased with high-definition endoscopy, 20–25 % of early stomach malignancies are still missed [32]. Narrow band imaging (NBI) and magnifying endoscopy together may provide very high accuracy, with sensitivity and specificity over 95 % [33,34]. he algorithm for the diagnosis of gastric cancer using magnifying endoscopy involves 1) the existence of demarcation lines, and 2) the presence of uneven micro-surfaces and/or microvascular patterns [35]. Previous studies have investigated the relationship between mucin phenotypes and histologic types [36–38]. Hyperplastic polyps are mostly seen to have weak or

Table 5
Association between magnifying endoscopic findings and mucin expression in early gastric cancers.

	Region area			Microsurface pattern					Microvascular pattern			
	Antrum-cancer (365)	Body-cancer (365)	p -value	Oval and/or tubular (207)	Papillary (45)	Destructive (34)	Absent (70)	p -value	Loop(86)	Fine network (74)	Corkscrew (186)	p -value
MUC2			0.055					0.115				0.021
Negative	205(56.16)	110(30.14)		188(90.82)	21(46.67)	15(44.11)	51(72.86)		74 (86.04)	40(54.05)	142(76.34)	
Positive	60(16.44)	255(69.86)		19(9.18)	24(53.33)	19(55.88)	19(27.14)		12 (13.95)	34(45.95)	44(23.66)	
MUC5AC			0.048					0.258				0.011
Negative	151(41.37)	61(16.71)		117(56.52)	35(77.78)	28(82.35)	15(21.43)		44 (51.16)	14(18.92)	28(15.05)	
Positive	114(31.23)	304(83.29)		90(43.47)	10(22.22)	6(17.65)	55(78.25)		42 (48.84)	60(81.08)	158(84.95)	
CD10			0.044					0.022				0.148
Negative	200(54.79)	215(58.91)		119(57.49)	11(24.44)	25(73.53)	11(15.71)		59 (68.60)	64(86.49)	177(95.16)	
Positive	165(45.21)	250(68.49)		88(42.51)	34(75.56)	9(26.47)	59(84.29)		17 (19.77)	10(13.15)	9(48.38)	

undetectable microvascular patterns when it comes to the enlarged NBI presentation of colonic tumors [34]. Adenomas are the primary cause of regular reticular microvascular patterns [33]. Intranucosal or superficial submucosal invasive carcinomas are the primary causes of irregular reticular microvascular patterns [39]. Deep submucosal invasive carcinomas are mostly characterized by reduced or loose microvascular patterns [35]. As a result, magnified NBI endoscopy may be used to determine the depth of infiltration in early colorectal cancer as well as to distinguish between adenomas and non-adenomatous lesions in the colon [40]. Based on the expression of mucus, differentiated stomach adenocarcinomas may be classified into intestinal or gastric phenotypes. It is now possible to discern between intestinal and gastric type differentiated adenocarcinomas with greater clinical significance because to recent developments in mucin histochemistry and immunohistochemistry [41]. The mucin phenotype has been shown by Kohei et al. to be a helpful marker for the management of gastric cancer in humans [42]. The expression of MUC1 and MUC2 phenotypes does not seem to correlate, in contrast to Lauren's classification [43]. More specifically, in gland-forming gastric cancer, the phrase "intestinal-type tumor" does not always refer to an immunohistochemical phenotype. At this time, it is unknown how mucin and pathogenic changes are related. During our analysis, we found a significant correlation between the pathogenic phenotype and mucin.

While dye-based and image-enhanced endoscopic methods have transformed the field of endoscopic diagnosis, regular endoscopy still heavily relies on traditional white light endoscopy for the detection of early gastric cancer (EGC). Nonetheless, during normal endoscopy, traditional white light endoscopy continues to be crucial in the detection of early gastric cancer (EGC) [44]. Narrow-band imaging (NBI) enables a thorough evaluation of vascular anatomy and surface characteristics, whereas color endoscopy shows the morphological characteristics of mucosal diseases by improving mucosal contrast [45,46]. When white-light imaging and sapphire-colored endoscopy provide positive diagnostic results for EGC, the lesion is well-defined and has uneven surface shape or color. The diagnostic precision of color endoscopy and white light imaging was further enhanced by magnified NBI [47]. There hasn't been a detailed investigation of changes to the mucosal surface of gastric adenomas and early gastric carcinomas as seen by enhanced-magnification endoscopy with acetic acid. Enhanced-magnification endoscopy has been reported by Kyosuke Tanaka et al. to be helpful in finding stomach cancers and assessing the degree of horizontal dissemination, particularly in tumors of the depressed type [48]. An early stomach cancer captioning model demonstrated satisfactory generalization, robustness, and interpretability in addition to showing promising captioning performance [49]. Consequently, it is critical for clinical outcomes to investigate the function of ME and microangiopathy in early gastric cancer.

The clinical and prognostic relevance of the mucin immunophenotype in gastric cancers is now the subject of a debate. The immunophenotype has been closely associated with a much worse prognosis and a higher risk of developing liver metastases after surgery [50]. On the other hand, the prognosis for the mucin intestinal phenotype has been shown to be much better [42]. In this work, we quantitatively analyzed early gastric cancer (EGC) and closely investigated the relationship between mucin and microangiopathy. Our results showed that, in comparison to lesions showing diverse patterns, those with a papillary MS pattern and those exhibiting a loop MV pattern expressed greater levels of CD10 and MUC2. Moreover, MUC2 expression was seen more often in lesions with a loop MV pattern than in lesions with other patterns. The background mucosa in multiple-type early gastric carcinomas and the instability of differentiated adenocarcinomas have been suggested as possible contributors to the increased neoplastic potential and recurrent nature of these carcinomas [51]. Furthermore, in 11.8 % of gastric-type differentiated adenocarcinomas, we found pure intestinal metaplasia, indicating that the mucin phenotype of an early-stage differentiated adenocarcinoma may not be a reliable indicator of the mucin type in the surrounding stomach mucosa [52]. In conclusion, ME is still the suggested screening method for EGC because of its.

This research has some limitations. Firstly, there was no lengthier follow-up, and the number of cases included was limited. In order to get more thorough data, future studies should improve both the sample size and the duration of follow-up. Second, it is difficult to determine which surgical technique is superior because this study focused primarily on the effectiveness of the NBI technique in treating early-stage gastric cancer. Future research should therefore compare the NBI technique with other techniques more thoroughly.

4. Conclusion

In conclusion, ME is still the recommended technique for screening EGC because of its efficiency and practicality. When it comes to detecting lesions in the stomach mucosa at an early stage, ME outperforms histology in terms of sensitivity and precision. With the use of this cutting-edge endoscopic equipment, healthcare providers may see gastric lesions more clearly and make links between the mucin phenotype, microsurface pattern, and microvascular pattern in EGC. Accurate identification of these patterns may facilitate future endoscopic excisions of the stomach mucosa in situations when histological investigation reveals the existence of a malignant tumor.

5. Materials and methods

5.1. Patients

The ethics committees of Chenzhou No. 1 People's Hospital gave their approval for this research. (ADWS25044-22). Every technique was used in compliance with all applicable laws and rules, including the Declaration of Helsinki. Between 2012 and 2020, Chenzhou No. 1 People's Hospital performed endoscopic submucosal dissection (ESD) on 402 patients who had been diagnosed with early gastric cancer (EGC). For these patients, three experienced endoscopists carried out ESD treatments using magnifying endoscopes equipped with NBI equipment. Before the trial, each patient was informed and had to sign a permission form.

5.2. ME

The Evis Lucera Spectrum system, created by Tokyo, Japan's Olympus Co., was used for video endoscopy. This system was made up of a GIF-H260Z magnifying video endoscope, a CV-260SL processor, and a CLV-260SL light source. A button on the video endoscope's control head made it easy to convert between the NBI and white light modes, allowing for up to 80× zoom magnifications. A soft hood (MB-46; Olympus Co.) was firmly fastened to the distal tip of the endoscope, preserving the focal distance, in order to guarantee clear vision for ME-NBI. Patients received 2–5 mg of midazolam for sedation throughout the examinations, although they remained aware. ME-NBI tests were conducted in the EGC zones to assess the MS and MV trends after routine monitoring. While MS patterns were characterized as oval and/or tubular, papillary, destructive, or nonexistent, MV patterns were classified as loop, fine network, or corkscrew. When lesions displayed both MS and MV patterns, the dominant pattern was used to classify the lesions [15,53].

5.3. Histological assessment

Either a gastrectomy or an endoscopic submucosal dissection (ESD) was carried out two weeks after the ME-NBI. Following resection, the samples were collected and stored in 10 % buffered formalin. Parallel slices of adjacent malignant and non-cancerous mucosa, each measuring 2 mm in thickness, were cut in order to perform histological investigation. After that, these slices underwent sectioning, staining with hematoxylin and eosin, and paraffin fixing. The specimens were then examined under a microscope in accordance with the Japanese Classification of Gastric Carcinomas standards to determine factors including tumor size, depth of invasion, ulceration presence, degree of differentiation, and lymphovascular invasion [54].

5.4. Mucin phenotype

Investigating the expression of MUC2 (Ccp58, 1:500; Novocastra Laboratories, Newcastle, UK), MUC5AC (CLH2, 1:500; Novocastra Laboratories), and CD10 (56C6, 1:100; Novocastra Laboratories) immunohistochemistry in cancer cells was the goal of the current investigation. To summarize, a series of increasing alcohol concentrations were used to deparaffinize and hydrate 5 μm thick tumor sections. The sections were treated to 10 mmol/L citrate buffer (pH 6.0) in a microwave oven for 10 min in order to retrieve the antigen. In order to prevent endogenous peroxidase activity, the slices were submerged in a 3 % H2O2/methanol solution. The sections were completely cleaned in phosphate-buffered solution after being treated with the primary antibodies. The sections were then subjected, using the Vectastain Elite ABC kit (Vector Laboratories, Burlingame, CA, USA), to the avidin-biotinylated horseradish peroxidase complex and biotinylated secondary antibody in that order. We observed antibody binding when we used Mayer's hematoxylin as a counterstain and the chromogen 3,3′-diaminobenzidine tetrachloride [55,56].

6. Microvessels

A positive immunostaining result meant that 10 % of the cancer cells were immunoreactive, as was previously reported. Here, we used a Laplacian operator to identify and measure microvessels. The microvessels were shown to have steep inclinations in the generated topographical map, and the degree of steepness was precisely assessed by the Laplacian operator. We added $I(x + i, y + j)I(x, y)$ for $i = 1, 0, 1$ and $j = 1, 0, 1$ in order to get the Laplacian value at coordinates (x, y). I(x,y) represents the blue reflectance intensity at the given image coordinates (x, y), and I(x,y) represents the matching Laplacian value. A group of points with a Laplacian value of at least 10 was referred to as a microvessel. In order to prevent overestimating or underestimating the segmented microvessels, we visually evaluated the Laplacian threshold and placed it at >9 or >11. Values outside of this range were deemed untrustworthy. To guarantee accuracy, out-of-focus or halation portions inside the area of interest were eliminated throughout the segmentation phase. An experienced endoscopist (N·H.) who was blind to the study's setting manually classified malignancy or the backdrop. Based on the segmented microvessels, the vascular bed area (represented as the percentage ratio of the vascular bed to the region of interest) and microvessel density (counts/mm2) were automatically computed, yielding a total of 19 vessels [57].

Microvessels were described as linear structures, and the item's geometry was represented by a collection of skeletonized pixels that included branching, connecting, end, and crossing points. The ratio of the total number of characteristic points (also called "the connected points") to the total number of pixels in the vascular bed prior to thinning was used to calculate the mean diameter of each microvessels [58].

6.1. Statistical analysis

This research aimed to investigate the effects of invasion depth, mucin phenotype, and histologic type on microsatellite instability (MS) and microvessel density (MV) patterns. Either the chi-square test or the Fisher exact test was used to compare the differences. IBM SPSS version 21.0 for Windows was used to conduct the statistical analysis (IBM Co., Armonk, NY, USA). To ascertain the statistical significance of the findings, a cutoff point of $p < 0.05$ was set [59–61].

Ethics statement

This study were approved by Ethics Committees of Chenzhou No. 1 People's Hospital. (ADWS25044-22). All methods were carried out in accordance with relevant guidelines and regulations in accordance with the Declaration of Helsinki.

Consent for publication

Not Applicable.

Data availability statement

The data used to support the findings of this study are included within the article.

Funding

This research was funded by Hunan Province Clinical Medical Technology Innovation Guidance Project in 2020(2020SK50307).

CRediT authorship contribution statement

Qian Zheng: Resources, Investigation, Funding acquisition, Formal analysis, Data curation, Conceptualization. **Yan Peng:** Writing – review & editing, Writing – original draft, Visualization, Validation, Supervision, Software, Resources, Methodology. **Han Xiong Liu:** Supervision, Software, Resources, Project administration, Methodology, Investigation. **Hui Qiu Cao:** Validation, Supervision, Software, Resources, Project administration, Methodology, Investigation. **Fang Fang Li:** Writing – original draft, Visualization, Validation, Supervision, Software.

Declaration of competing interest

The authors declare the following financial interests/personal relationships which may be considered as potential competing interests:Qian zhen reports was provided by Chenzhou No.1 People's Hospital. Qian zhen reports a relationship with Chenzhou No.1 People's Hospital that includes: board membership, consulting or advisory, employment, equity or stocks, funding grants, non-financial support, paid expert testimony, speaking and lecture fees, and travel reimbursement. none If there are other authors, they declare that they have no known competing financial interests or personal relationships that could have appeared to influence the work reported in this paper.

Acknowledgments

We would like to thank all participants and our hospital.

References

[1] E.C. Smyth, et al., Gastric cancer, Lancet 396 (10251) (2020) 635–648.
[2] N.Y. Chia, P. Tan, Molecular classification of gastric cancer, Ann. Oncol. 27 (5) (2016) 763–769.
[3] C. Oliveira, et al., Familial gastric cancer: genetic susceptibility, pathology, and implications for management, Lancet Oncol. 16 (2) (2015) e60–e70.
[4] M. Muto, et al., Magnifying endoscopy simple diagnostic algorithm for early gastric cancer (MESDA-G), Dig. Endosc. 28 (4) (2016) 379–393.
[5] M. Del Fabbro, et al., Magnification devices for endodontic therapy, Cochrane Database Syst. Rev. 2015 (12) (2015) Cd005969.
[6] V. Zimmer, K. Emrich, High-quality endoscopic perspective on pseudomelanosis ilei: underwater, magnified and image-enhanced, Clin Res Hepatol Gastroenterol 45 (4) (2021) 101643.
[7] Y.J. Hsiao, et al., Application of artificial intelligence-driven endoscopic screening and diagnosis of gastric cancer, World J. Gastroenterol. 27 (22) (2021) 2979–2993.
[8] J.C. Byrd, R.S. Bresalier, Mucins and mucin binding proteins in colorectal cancer, Cancer Metastasis Rev. 23 (1–2) (2004) 77–99.
[9] V.R. Kohout, C.L. Wardzala, J.R. Kramer, Synthesis and biomedical applications of mucin mimic materials, Adv. Drug Deliv. Rev. 191 (2022) 114540.
[10] D.H. Wi, J.H. Cha, Y.S. Jung, Mucin in cancer: a stealth cloak for cancer cells, BMB Rep 54 (7) (2021) 344–355.
[11] B. Demouveaux, et al., Gel-forming mucin interactome drives mucus viscoelasticity, Adv. Colloid Interface Sci. 252 (2018) 69–82.
[12] Y. Adachi, et al., Microvascular architecture of early gastric carcinoma. Microvascular-histopathologic correlates, Cancer 72 (1) (1993) 32–36.
[13] K. Yao, et al., Novel zoom endoscopy technique for visualizing the microvascular architecture in gastric mucosa, Clin. Gastroenterol. Hepatol. 3 (7 Suppl 1) (2005) S23–S26.
[14] M. Kobayashi, et al., Mucin phenotype and narrow-band imaging with magnifying endoscopy for differentiated-type mucosal gastric cancer, J. Gastroenterol. 46 (9) (2011) 1064–1070.
[15] K.S. Ok, et al., Magnifying endoscopy with narrow band imaging of early gastric cancer: correlation with histopathology and mucin phenotype, Gut Liver 10 (4) (2016) 532–541.
[16] S. Akiyama, et al., Evolving roles of magnifying endoscopy and endoscopic resection for neoplasia in inflammatory bowel diseases, World J. Gastrointest. Oncol. 14 (3) (2022) 646–653.
[17] Y. Sano, et al., Narrow-band imaging (NBI) magnifying endoscopic classification of colorectal tumors proposed by the Japan NBI Expert Team, Dig. Endosc. 28 (5) (2016) 526–533.
[18] J.L. Teh, et al., Recent advances in diagnostic upper endoscopy, World J. Gastroenterol. 26 (4) (2020) 433–447.
[19] D. Libânio, et al., Endoscopic submucosal dissection techniques and technology: European society of gastrointestinal endoscopy (ESGE) technical review, Endoscopy 55 (4) (2023) 361–389.
[20] B. Weusten, et al., Diagnosis and management of barrett esophagus: European society of gastrointestinal endoscopy (ESGE) guideline, Endoscopy 55 (12) (2023) 1124–1146.
[21] N.L. Chai, et al., Magnifying endoscopy in upper gastroenterology for assessing lesions before completing endoscopic removal, World J. Gastroenterol. 18 (12) (2012) 1295–1307.
[22] M. Nishio, et al., Magnifying endoscopy is useful for tumor border diagnosis in ulcerative colitis patients, Dig. Liver Dis. 54 (6) (2022) 812–818.
[23] H. Oh, et al., Magnifying endoscopy with narrow-band imaging for gastric heterotopic pancreas, Endosc. Int. Open 6 (3) (2018) E369–e375.
[24] K. Yao, et al., Novel magnified endoscopic findings of microvascular architecture in intramucosal gastric cancer, Gastrointest. Endosc. 56 (2) (2002) 279–284.

[25] T. Nakayoshi, et al., Magnifying endoscopy combined with narrow band imaging system for early gastric cancer: correlation of vascular pattern with histopathology (including video), Endoscopy 36 (12) (2004) 1080–1084.
[26] H. Sunakawa, et al., Relationship between the microvascular patterns observed by magnifying endoscopy with narrow-band imaging and the depth of invasion in superficial pharyngeal squamous cell carcinoma, Esophagus 18 (1) (2021) 111–117.
[27] H. Ueyama, et al., Dynamic diagnosis of early gastric cancer with microvascular blood flow rate using magnifying endoscopy (with video): a pilot study, J. Gastroenterol. Hepatol. 36 (7) (2021) 1927–1934.
[28] K. Yao, G.K. Anagnostopoulos, K. Ragunath, Magnifying endoscopy for diagnosing and delineating early gastric cancer, Endoscopy 41 (5) (2009) 462–467.
[29] W.F. Chen, et al., [Clinical value of different magnifying chromoendoscopy methods in screening gastric precancerous lesions and early cancers], Zhonghua Wei Chang Wai Ke Za Zhi 15 (7) (2012) 662–667.
[30] H. Yu, et al., Magnifying narrow-band imaging endoscopy is superior in diagnosis of early gastric cancer, World J. Gastroenterol. 21 (30) (2015) 9156–9162.
[31] H. Liu, et al., Evaluating the diagnoses of gastric antral lesions using magnifying endoscopy with narrow-band imaging in a Chinese population, Dig. Dis. Sci. 59 (7) (2014) 1513–1519.
[32] M. Kaise, Advanced endoscopic imaging for early gastric cancer, Best Pract. Res. Clin. Gastroenterol. 29 (4) (2015) 575–587.
[33] T.T. Law, et al., Helicobacter pylori-negative gastric mucosa-associated lymphoid tissue lymphoma: magnifying endoscopy findings, Hong Kong Med. J. 21 (2) (2015) 183–186.
[34] H. Uchima, K. Yao, Endoscopic microanatomy of the normal gastrointestinal mucosa with narrow band technology and magnification, Gastroenterol. Hepatol. 42 (2) (2019) 117–126.
[35] I. Hirata, et al., Usefulness of magnifying narrow-band imaging endoscopy for the diagnosis of gastric and colorectal lesions, Digestion 85 (2) (2012) 74–79.
[36] T. Namikawa, K. Hanazaki, Mucin phenotype of gastric cancer and clinicopathology of gastric-type differentiated adenocarcinoma, World J. Gastroenterol. 16 (37) (2010) 4634–4639.
[37] P. Ramalingam, Immunophenotypic Morphologic, Molecular features of epithelial ovarian cancer, Oncology (Williston Park) 30 (2) (2016) 166–176.
[38] T. Ueo, et al., Histologic differentiation and mucin phenotype in white opaque substance-positive gastric neoplasias, Endosc. Int. Open 3 (6) (2015) E597–E604.
[39] O. Kikuchi, et al., Narrow-band imaging for the head and neck region and the upper gastrointestinal tract, Jpn. J. Clin. Oncol. 43 (5) (2013) 458–465.
[40] S. Oka, et al., Clinical usefulness of narrow band imaging magnifying classification for colorectal tumors based on both surface pattern and microvessel features, Dig. Endosc. 23 (Suppl 1) (2011) 101–105.
[41] L. Kennedy, et al., Secretin alleviates biliary and liver injury during late-stage primary biliary cholangitis via restoration of secretory processes, J. Hepatol. 78 (1) (2023) 99–113.
[42] K. Wakatsuki, et al., Clinicopathological and prognostic significance of mucin phenotype in gastric cancer, J. Surg. Oncol. 98 (2) (2008) 124–129.
[43] V. Barresi, et al., Relationship between immunoexpression of mucin peptide cores MUC1 and MUC2 and Lauren's histologic subtypes of gastric carcinomas, Eur. J. Histochem. 50 (4) (2006) 301–309.
[44] C. Gómez Díez, et al., The role of magnification endoscopy in the early diagnosis of gastric signet ring cell carcinoma, Rev. Esp. Enferm. Dig. 116 (2023).
[45] N. Soma, Diagnosis of Helicobacter pylori-related chronic gastritis, gastric adenoma and early gastric cancer by magnifying endoscopy, J Dig Dis 17 (10) (2016) 641–651.
[46] N. Uedo, K. Yao, Endoluminal diagnosis of early gastric cancer and its precursors: bridging the gap between endoscopy and pathology, Adv. Exp. Med. Biol. 908 (2016) 293–316.
[47] V. Baptista, A. Singh, W. Wassef, Early gastric cancer: an update on endoscopic management, Curr. Opin. Gastroenterol. 28 (6) (2012) 629–635.
[48] K. Tanaka, et al., Features of early gastric cancer and gastric adenoma by enhanced-magnification endoscopy, J. Gastroenterol. 41 (4) (2006) 332–338.
[49] L. Gong, et al., Automatic captioning of early gastric cancer using magnification endoscopy with narrow-band imaging, Gastrointest. Endosc. 96 (6) (2022) 929–942.e6.
[50] O.J. Lee, et al., The prognostic significance of the mucin phenotype of gastric adenocarcinoma and its relationship with histologic classifications, Oncol. Rep. 21 (2) (2009) 387–393.
[51] A. Kabashima, et al., Gastric or intestinal phenotypic expression in the carcinomas and background mucosa of multiple early gastric carcinomas, Histopathology 37 (6) (2000) 513–522.
[52] R. Aihara, et al., Clinical significance of mucin phenotype, beta-catenin and matrix metalloproteinase 7 in early undifferentiated gastric carcinoma, Br. J. Surg. 92 (4) (2005) 454–462.
[53] T. Yoshida, et al., The clinical meaning of a nonstructural pattern in early gastric cancer on magnifying endoscopy, Gastrointest. Endosc. 62 (1) (2005) 48–54.
[54] Japanese classification of gastric carcinoma: 3rd English edition, Gastric Cancer 14 (2) (2011) 101–112.
[55] D.Y. Park, et al., Adenomatous and foveolar gastric dysplasia: distinct patterns of mucin expression and background intestinal metaplasia, Am. J. Surg. Pathol. 32 (4) (2008) 524–533.
[56] G. Ha Kim, et al., CDX2 expression is increased in gastric cancers with less invasiveness and intestinal mucin phenotype, Scand. J. Gastroenterol. 41 (8) (2006) 880–886.
[57] Jr. F.W. Billmeyer, in: Gunter Wyszecki, W.S. Stiles (Eds.), Color Science: Concepts and Methods, Quantitative Data and Formulae, second ed., John Wiley and Sons, New York, 1982, p. 950, *pp. Price: $75.00.* 1983. **8**(4): pp. 262–263.
[58] J. Parker, Algorithms for Image Processing and Computer Vision, 1997.
[59] T. Radhika, et al., Analysis of markovian jump stochastic cohen–grossberg BAM neural networks with time delays for exponential input-to-state stability, Neural Process. Lett. 55 (8) (2023) 11055–11072.
[60] Y. Cao, et al., Input-to-state Stability of Stochastic Markovian Jump Genetic Regulatory Networks, 2023.
[61] M Tamil Thendral, TR Ganesh Babu, Synchronization of Markovian jump neural networks for sampled data control systems with additive delay components: Analysis of image encryption technique, Math Methods Appl Sci (2022). https://doi.org/10.1002/mma.8774.